Published in final edited form as:
Nanotechnology. 2007 July ; 18(5): 055102–. doi:10.1088/0957-4484/18/5/055102.

Magnetic/luminescent core/shell particles synthesized by spray pyrolysis and their application in immunoassays with internal standard

Dosi Dosev[1], **Mikaela Nichkova**[2], **Randy K Dumas**[3], **Shirley J Gee**[2], **Bruce D Hammock**[2], **Kai Liu**[3], and **Ian M Kennedy**[1]

1 *Department of Mechanical and Aeronautical Engineering, University of California Davis, One Shields Avenue, Davis, CA 95616, USA*

2 *Department of Entomology, University of California Davis, One Shields Avenue, Davis, CA 95616, USA*

3 *Department of Physics, University of California Davis, One Shields Avenue, Davis, CA 95616, USA*

Abstract

Many types of fluorescent nanoparticles have been investigated as alternatives to conventional organic dyes in biochemistry; magnetic beads also have a long history of biological applications. In this work we apply flame spray pyrolysis in order to engineer a novel type of nanoparticle that has both luminescent and magnetic properties. The particles have magnetic cores of iron oxide doped with cobalt and neodymium and luminescent shells of europium-doped gadolinium oxide ($Eu:Gd_2O_3$). Measurements by vibrating sample magnetometry showed an overall paramagnetic response of these composite particles. Luminescence spectroscopy showed spectra typical of the Eu ion in a Gd_2O_3 host—a narrow emission peak centred near 615 nm. Our synthesis method offers a low-cost, high-rate synthesis route that enables a wide range of biological applications of magnetic/luminescent core/shell particles. Using these particles we demonstrate a novel immunoassay format with internal luminescent calibration for more precise measurements.

1. Introduction

A large variety of nanoparticles with different properties have been subject to intense research focused on their synthesis, characterization and application in biochemistry [1]. Fluorescent nanoparticles have been demonstrated as promising alternatives to widely used organic fluorescent dyes [2]. Quantum dots [3,4], dye-doped silica [5], chelate-doped polystyrene [6] and lanthanide oxides [7,8] each offer unique advantages and find different applications as fluorescent labels in biotechnology such as cell staining, molecular recognition, immunoassays [3,9-13], visualization of DNA and protein microarrays [14,15].

Core/shell structured magnetic nanoparticles are currently of interest in a wide variety of applications. For example, Fe/Au core/shell structured nanoparticles [16,17], due to the possibility of remote magnetic manipulation [18], may be used in biological applications as magnetic resonance imaging (MRI) agents [19,20], cell tagging and sorting [21] and targeted drug delivery [22] (for reviews see [23,24]).

The combination of magnetic and fluorescent properties is a new powerful tool allowing manipulation by magnetic fields and visualization/detection by fluorescence. There are

E-mail: imkennedy@ucdavis.edu

commercially available tools and automatic instruments for manipulating magnetic particles and for detecting a variety of fluorescent labels over the entire visible spectrum.

Recently, several groups reported the successful synthesis of particles that possess both fluorescent and magnetic properties. In most of these works, colloidal solution techniques were employed. Lu *et al* [25] and Levy *et al* [26] coated iron oxide particles with silica shells containing organic dyes which provided the fluorescent properties of the nanoparticles. Sahoo *et al* [27] employed covalent binding of organic dyes on the surface of magnetite particles. Using covalent binding, Wang *et al* [28] formed a fluorescent shell of quantum dots on polymer-coated iron oxide beads, while Mulvaney *et al* [29] incorporated organic dyes and quantum dots into the polystyrene shell of magnetic beads. Lu *et al* [30] formed a shell of up-converting phosphor (ytterbium and erbium co-doped sodium yttrium fluoride) on an iron oxide core that made use of the luminescent properties of the lanthanide ions.

In most of the cases, the synthesis of particles with magnetic and fluorescent properties is complicated and expensive. An additional drawback is that organic dyes have broad emission spectra and poor photostability. An efficient and low-cost method for synthesis of magnetic/fluorescent particles would be highly beneficial for applications that demand significant amounts of reagents and are economical—environmental monitoring for bioterror agents is a good example. A low-cost synthesis route would allow improvements in biotechnologies and facilitate the creation of new widely applicable biochemical protocols.

Here we report the synthesis and the properties of magnetic/luminescent core/shell particles consisting of magnetic cores of iron oxide doped with cobalt and neodymium (Nd:Co:Fe_2O_3) which are encapsulated in luminescent shells of europium-doped gadolinium oxide (Eu:Gd_2O_3). Cobalt [31] and neodymium [32] were shown to improve the magnetic properties of iron oxides. In addition, doping of Eu ions into the Gd_2O_3 matrix gives unique luminescent properties [33,34]. We employ flame spray pyrolysis as a cost-effective, high throughput and versatile synthesis method, allowing a variety of doped materials to be obtained. In addition, we demonstrate the application of the particles in a new format for a quantitative magnetic immunoassay with an internal luminescent standard.

2. Synthesis and characteristics of magnetic/luminescent core/shell particles

2.1. Synthesis and properties of the magnetic cores

Magnetic particles of Nd:Co:Fe_2O_3 mixed oxide were obtained by a spray pyrolysis method, previously reported for synthesis of Eu:Y_2O_3 nanoparticles [35]. Briefly, an ethanol solution containing $Fe(NO_3)_3$, $Co(NO_3)_2$ and $Nd(NO_3)_3$ was sprayed into a hydrogen diffusion flame through a nebulizer. The flame was formed by an H_2 flow at 2 l min^{-1} and an air co-flow at 10 l min^{-1}, surrounding the outlet of the nebulizer. A flame temperature of about 2000°C was measured. Pyrolysis of the precursor solution within the flame yielded Nd:Co:Fe_2O_3 nanoparticles. A cold finger was used for collecting the particles thermophoretically. The production rate of this synthesis procedure was about 400–500 mg h^{-1}. The ratio between Fe/Co/Nd salts was optimized experimentally to achieve the best magnetic characteristics.

Figure 1 shows the magnetic hysteresis loops of Co:Fe_2O_3 composite nanoparticles for powders obtained from liquid precursors with different mixing ratios of Co and Fe. The applied external magnetic field was in the range of ±18 kOe. Pure Fe_2O_3 shows little magnetic hysteresis and small saturation magnetization. We attribute this to the high temperature during the synthesis process that does not favour the formation of magnetic γ-Fe_2O_3. However, adding $Co(NO_3)_3$ to the precursor mixture helped to improve the magnetic response, reaching maximum saturation magnetization with a Fe/Co ratio of 80/20. Further addition of Co to the precursor did not lead to improvement but to a decreasing of the saturation magnetization (see

ratios Fe/Co of 65/35 and 65/45 in figure 1). Adding a small amount of $Nd(NO_3)_3$ to the precursor mixture helped to further increase the magnetization as shown in figure 1. The powder containing Nd reached about 25–30% higher saturation magnetization than the one without Nd. Adding larger amounts of Nd precursor did not improve the magnetization (data not shown).

2.2. Synthesis and properties of the core/shell magnetic luminescent particles

The Co:Nd:Fe_2O_3 powder with a Fe:Co:Nd ratio of 80:20:5 was used for the synthesis of core/shell particles, building the luminescent Eu:Gd_2O_3 shell via a second spray pyrolysis process. 10 mg of Co:Nd:Fe_2O_3 nanoparticles were dispersed in 50 ml ethanol containing 20 mM Eu $(NO_3)_3$ and 80 mM $Gd(NO_3)_3$. The solution was subjected to an ultrasonic bath for 30 min in order to break any weak agglomerates. Afterwards it was sprayed through the hydrogen flame (figure 2). Gas and liquid flow rates were the same as described above. Each droplet of the formed spray contained solid magnetic particles and liquid precursors of Eu and Gd in ethanol. As a result, a composite particle containing magnetic cores and Eu:Gd_2O_3 luminescent shell was formed from each droplet in the flame. The Nd:Co:Fe_2O_3 nanoparticles in this case served as seeds for the formation of new particles in the spray. Other authors used seeds in a similar way for the synthesis of Eu:Y_2O_3 nanoparticles by spray pyrolysis [36].

Analysis with a transmission electron microscope (TEM) revealed that most of the synthesized particles were in the size range between 200 nm and 1 μm depending on the number and the size of the embedded primary Co:Nd:Fe_2O_3 particles. A representative TEM image of a core/shell particle can be seen in figure 3. The image reveals the external shape of the particle as well as its internal morphology. The particle has an irregular form and an overall diameter of about 400 nm. Several primary Co:Nd:Fe_2O_3 particles of different sizes can be distinguished, all of them embedded in a shell with a thickness of 10–20 nm.

The magnetic characteristics of the core (Co:Nd:Fe_2O_3) and the shell (Eu:Gd_2O_3) materials are compared to those of the final core/shell particles in figure 4(a). While the cores exhibit ferromagnetic behaviour, the core/shell particles after the second spray pyrolysis display a paramagnetic response. The aligned magnetization of the core/shell particles reaches nearly the same value as the ferromagnetic cores under an external magnetic field of ±18 kOe. In comparison, the magnetization of the shell material itself is much smaller. Note that in all cases the background contribution is negligible. This change of the magnetic characteristics from ferromagnetic core to paramagnetic core/shell particles can be attributed to a reduction or phase transformation of the magnetic core phase during the second spray pyrolysis process.

Figure 4(b) shows the luminescent emission spectrum of the synthesized core/shell particles which is typical for the shell material Eu:Gd_2O_3. Under UV excitation at 260 nm, the particles with Eu:Gd_2O_3 shell emitted red luminescence with a narrow peak centred at 615 nm that was identical to the spectrum we recently reported for Eu:Gd_2O_3 nanoparticles [15]. The compatibility of Gd_2O_3 with the proposed synthesis process introduces the possibility for a variety of luminescent spectra to be achieved by using different lanthanides such as Tb, Sm or Dy for doping [34].

We have performed x-ray diffraction studies of the primary obtained Nd:Co:Fe_2O_3 powder and the final core/shell particles in order to clarify the origin of the observed changes in the magnetic properties. The XRD spectrum of the primary magnetic particles reveal the presence of FeO_4 iron oxide along with other phases (figure 5(a)). The XRD spectrum of the secondary core/shell particles (figure 5(b)) shows a pattern close to the monoclinic Gd_2O_3 phase (figure 5(d)), which is in agreement with recently published results [33]. Some additional peaks (e.g. at $2\theta = 24.7°, 29.7°, 45.3°$) coincide with strong peaks of Fe_2O_3 (figure 5(c)). This leads to the conclusion that the core materials are changed (e.g. oxidized) during the second synthesis stage.

The final core/shell particles were successfully separated from an aqueous solution by a commercially available permanent magnet for biochemical purposes, as shown in figure 6. Initially, the particles that were suspended in water were attracted to the magnet and stuck to the glass wall (figure 6(a)). Afterwards, the water was pulled out of the tube leaving the particles in the tube (figure 6(b)). The attractive force that the particles experienced was sufficiently strong to prevent re-entrainment by the liquid flow during the removal of the water. This simple experiment demonstrates the applicability of the synthesized particles for separation purposes in biochemical protocols.

3. Immunoassay with internal calibration standard performed on the surface of the core/shell particles

Using the magnetic luminescent nanoparticles, we developed a magnetic immunoassay in which the luminescence of the magnetic particles was used for internal calibration of the assay. As a proof of concept, we performed a competitive immunoassay for rabbit IgG where the labelled antigen (rabbit Ig-Alexa Fluor 350) and the analyte (rabbit IgG) in the solution compete for the antibody (anti-rabbit IgG) immobilized on the nanoparticle surface.

3.1. Biofunctionalization of the core/shell particles

The magnetic luminescent nanoparticles were coated with anti-rabbit IgG via spontaneous physical adsorption according to our previously reported procedure for the biofunctionalization of Eu:Gd_2O_3 nanoparticles [7]. Briefly, a suspension of the nanoparticles in 25 mM phosphate buffer, pH = 7, was incubated overnight in the antibody solution in a rotating mill at room temperature. The particles were extracted from the solution on a magnetic rack and washed three times. After that their surface was blocked with BSA to ensure that no bare particle surface remained.

The concentrations of the coating antibody and labelled antigen were optimized in a titration experiment where 1 mg of particles, coated with anti-rabbit IgG in the concentration range of 10–500 μg mg^{-1} particles, were incubated for 1 h with different concentrations of rabbit IgG-Alexa Fluor 350. Negative controls were performed with magnetic nanoparticles coated with sheep IgG. After magnetic extraction, the nanoparticles were resuspended in 100 μl of PBS and the fluorescence of the resulting complex was measured on a Spectramax M2 microplate reader (Molecular Devices, Sunnyvale, CA). Both Eu:Gd_2O_3 and Alexa Fluor 350 were excited at 350 nm and their emission spectra were detected in the interval 430–670 nm. Figure 7 represents the emission spectrum corresponding to 100 μg antibody/mg nanoparticles and 20 μg ml^{-1} rabbit IgG-Alexa Fluor 350. The intensity of Alexa Fluor 350 emission (at 445 nm) is proportional to the amount of labelled antigen bound to the particle surface while the intensity of Eu emission (at 615 nm) is related to the number of particles, and hence number of antibodies —the Eu signal serves as an internal standard.

A typical titration curve representing the saturation of the immobilized antibody by the labelled antigen is presented in figure 8. The absolute measured signal of Alexa 350 is compared to the normalized signal (intensity ratio Alexa 350/Eu). Although the two curves show the same tendency toward saturation, using the internal fluorescent standard generates much smoother curves and more precise measurement. This approach eliminates the error due to possible variability in the magnetic particle extraction. The measured signal is relative instead of absolute, with the Eu signal as a measure for the amount of particles and antibodies that are interrogated in the plate reader. In this way, the intrinsic luminescence of the magnetic nanoparticles serves as an internal standard in the quantitative immunoassay. For the competitive magnetic immunoassay, the amount of coating antibody and the concentration of the labelled antigen were selected to generate a high signal-to-noise ratio. As a result of the

titration experiments, we chose a coating antibody concentration of 100 μg antibody/mg nanoparticles and a concentration of rabbit IgG-Alexa Fluor 350 corresponding to 70% saturation of the capture antibody binding sites (about 20 μg ml^{-1}). This internal standard procedure will facilitate the development and improvement of a variety of novel sensor formats where the separation and recovery of magnetic particles is not absolutely quantitative.

3.2. Competitive immunoassay

A competitive magnetic immunoassay for detection of rabbit IgG (target analyte) was performed on the functionalized particle surface. Half a mg of anti-rabbit IgG-coated magnetic nanoparticles was pre-incubated with the target analyte in 1 ml of 0.2% BSA/PBS for 1 h in a rotating mill at room temperature. After magnetic separation, the particles were incubated with a solution of 20 μg ml^{-1} of rabbit IgG-Alexa Fluor 350 for 1 h at room temperature. During this incubation the labelled IgG bound to the available binding sites on the particle surface. The amount of labelled antigen bound on the nanoparticle surface is inversely proportional to the amount of analyte in the sample during the first incubation. Finally the particles were extracted magnetically from the solution. In the detection step, the amount of bound, labelled antigen was quantified by the ratio between the intensities of Alexa 350 and Eu:Gd_2O_3. The measured rabbit IgG competitive curve is presented in figure 9. The parameters for the sigmoidal fit are as follows: IC50 = 2 μg ml^{-1}, slope = −0.75, R^2 = 0.96. The LOD is ~0.1 μg ml^{-1}. It is worth noticing the small standard deviations that emphasize the advantage of using an internal luminescent standard. Optimization of the assay sensitivity was not the subject of this work. Our main goal was to demonstrate that the novel luminescent magnetic nanoparticles can be successfully applied to assays based on magnetic separation and used as a substrate for the immobilization of biological receptors. This immunoassay method is potentially attractive for clinical applications in which magnetic separation is used.

An important advantage of the proposed immunoassay on the particle surface is that it permits any type of fluorophore to be used as a secondary label. The intensity of the secondary label can be tuned by varying the amount of used core/shell particles, and therefore the amount of surface binding sites. This way, more particles (larger surface) can be used in order to obtain higher intensity of the secondary label which will not change the quantitative (ratiometric) measurement but will increase the sensitivity. In addition, the large number of particles used in the assay avoids error from particle size non-uniformity—the size distribution of the particles does not change and hence the total particle surface area per unit mass of particles is constant. The sharp emission spectrum and long lifetime of Eu^{3+} ions (about 1 ms) allows us to use any other fluorophores as secondary labels such as quantum dots or polystyrene beads. Even if their spectra overlap with that of the Eu^{3+} ion, the signal from the long-lifetime Eu^{3+} ions can be resolved with time-gated detection.

4. Conclusions

We have demonstrated a novel method for the synthesis of core/shell particles that possess both magnetic and luminescent properties. The synthesis consists of two stages fully based on spray pyrolysis which offers a high-rate and low-cost fabrication route for oxides. In addition, the flexibility of spray pyrolysis allowed us to obtain optimized three-component magnetic oxide as a core material. A fluorescent shell was built around the magnetic cores via a second spray pyrolysis step. The magnetic properties of the synthesized particles enable their separation from aqueous solution and make them suitable for separation applications in biochemistry. The luminescence makes possible their detection and identification by means of luminescent spectroscopy. This bi-functionality allowed us to develop a new immunoassay format with an internal luminescent standard, thus eliminating the experimental error inherent in particle extraction and measurement of absolute organic dye fluorescence intensities. The

developed protocol is applicable also with other fluorophores as secondary labels such as quantum dots, polystyrene beads, etc., with any type of spectral properties, providing the possibility to tune the intensity of those labels in accordance with the specifics of the detection system. The magnetic luminescent nanoparticles synthesized in this work have the potential for a variety of biological applications, including magnetic separation and detection of cells, bacteria and viruses.

Acknowledgments

The authors wish to acknowledge the support of the National Science Foundation, Grant DBI-0102662, the Superfund Basic Research Program with Grant 5P42ES04699 from the National Institute of Environmental Health Sciences, NIEHS, the support of the Cooperative State Research, Education, and Extension Service, US Department of Agriculture, under Award No 05-35603-16280, American Chemical Society—Petroleum Research Fund under Award No 43637-AC10 and the Alfred P Sloan Foundation.

References

1. Alivisatos P. Nat. Biotechnol 2004;22:47–52. [PubMed: 14704706]
2. Seydack M. Biosensors Bioelectron 2005;20:2454–69.
3. Parak WJ, Gerion D, Pellegrino T, Zanchet D, Micheel C, Williams SC, Boudreau R, Le Gros MA, Larabell CA, Alivisatos AP. Nanotechnology 2003;14:R15–27.
4. Jaiswal JK, Simon SM. Trends Cell Biol 2004;14:497–504. [PubMed: 15350978]
5. Tan MQ, Wang GL, Hai XD, Ye ZQ, Yuan JL. J. Mater. Chem 2004;14:2896–901.
6. Harma H, Soukka T, Lovgren T. Clin. Chem 2001;47:561–8. [PubMed: 11238312]
7. Nichkova M, Dosev D, Perron R, Gee SJ, Hammock BD, Kennedy IM. Anal. Bioanal. Chem 2006;384:631–7. [PubMed: 16416096]
8. Nichkova M, Dosev D, Gee SJ, Hammock BD, Kennedy IM. Anal. Chem 2005;77:6864–73. [PubMed: 16255584]
9. Tan WH, Wang KM, He XX, Zhao XJ, Drake T, Wang L, Bagwe RP. Med. Res. Rev 2004;24:621–38. [PubMed: 15224383]
10. Ye ZQ, Tan MQ, Wang GL, Yuan JL. Anal. Chem 2004;76:513–8. [PubMed: 14750841]
11. Ye ZQ, Tan MQ, Wang GL, Yuan JL. J. Mater. Chem 2004;14:851–6.
12. Huhtinen P, Soukka T, Lovgren T, Harma H. J. Immun. Meth 2004;294:111–22.
13. Feng J, Shan GM, Maquieira A, Koivunen ME, Guo B, Hammock BD, Kennedy IM. Anal. Chem 2003;75:5282–6.
14. Gerion D, Chen FQ, Kannan B, Fu AH, Parak WJ, Chen DJ, Majumdar A, Alivisatos AP. Anal. Chem 2003;75:4766–72. [PubMed: 14674452]
15. Dosev D, Nichkova M, Liu MZ, Guo B, Liu GY, Hammock BD, Kennedy IM. J. Biomed. Opt 2005;10:064006–064001/064007. [PubMed: 16409071]
16. Cho SJ, Kauzlarich SM, Olamit J, Liu K, Grandjean F, Rebbouh L, Long GJ. J. Appl. Phys 2004;95:6804–6.
17. Yoon TJ, Kim JS, Kim BG, Yu KN, Cho MH, Lee JK. Angew. Chem. Int. Edn 2005;44:1068–71.
18. Wirix-Speetjens R, De Boeck J. IEEE Trans. Magn 2004;40:1944–6.
19. Oswald P, Clement O, Chambon C, Schoumanclaeys E, Frija G. Magn. Reson. Imag 1997;15:1025–31.
20. Kim DK, Zhang Y, Voit W, Kao KV, Kehr J, Bjelke B, Muhammed M. Scr. Mater 2001;44:1713–7.
21. Niemeyer CM. Angew. Chem. Int. Edn 2001;40:4128–58.
22. Zahn M. J. Nanoparticle Res 2001;3:73–8.
23. Jain KK. Expert Rev. Mol. Diagnostics 2003;3:153–61.
24. Hasan R, Bernard A, Ciccotelli J, Martin P. Safety Sci 2003;41:155–79.
25. Lu Y, Yin YD, Mayers BT, Xia YN. Nano Lett 2002;2:183–6.
26. Levy L, Sahoo Y, Kim KS, Bergey EJ, Prasad PN. Chem. Mater 2002;14:3715–21.

27. Sahoo Y, Goodarzi A, Swihart MT, Ohulchanskyy TY, Kaur N, Furlani EP, Prasad PN. J. Phys. Chem. B 2005;109:3879–85. [PubMed: 16851439]
28. Wang DS, He JB, Rosenzweig N, Rosenzweig Z. Nano Lett 2004;4:409–13.
29. Mulvaney SP, Mattoussi HM, Whitman LJ. BioTechniques 2004;36:602–9. [PubMed: 15088378]
30. Lu HC, Yi GS, Zhao SY, Chen DP, Guo LH, Cheng J. J. Mater. Chem 2004;14:1336–41.
31. Montemayor SM, Garcia-Cerda LA, Torres-Lubian JR. Mater. Lett 2005;59:1056–60.
32. Sinnecker EHCP, Gama S, Ribeiro CA. J. Appl. Phys 1991;70:6480–2.
33. Goldys EM, Drozdowicz-Tomsia K, Jinjun S, Dosev D, Kennedy IM, Yatsunenko S, Godlewski M. J. Am. Chem. Soc 2006;128:14498–505. [PubMed: 17090033]
34. Gordon WO, Carter JA, Tissue BM. J. Lumin 2004;108:339–42.
35. Dosev D, Guo B, Kennedy IM. J. Aerosol Sci 2006;37:402–12.
36. Kang YC, Roh HS, Park SB. Adv. Mater 2000;12:451–3.

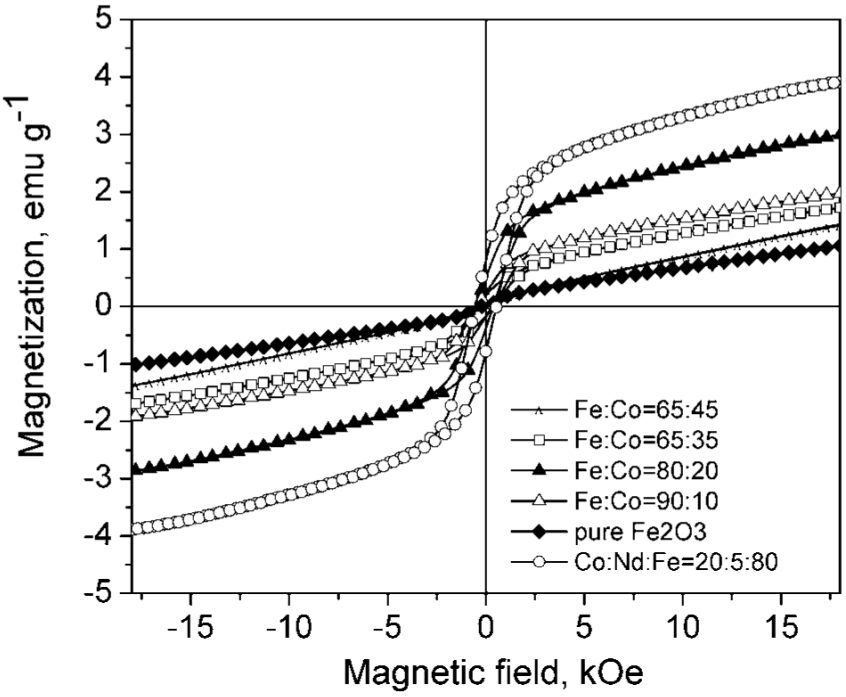

Figure 1.
Magnetic characteristics of Co:Fe_2O_3 and Co:Nd:Fe_2O_3 powders synthesized by spray pyrolysis with different partial Co, Nd.

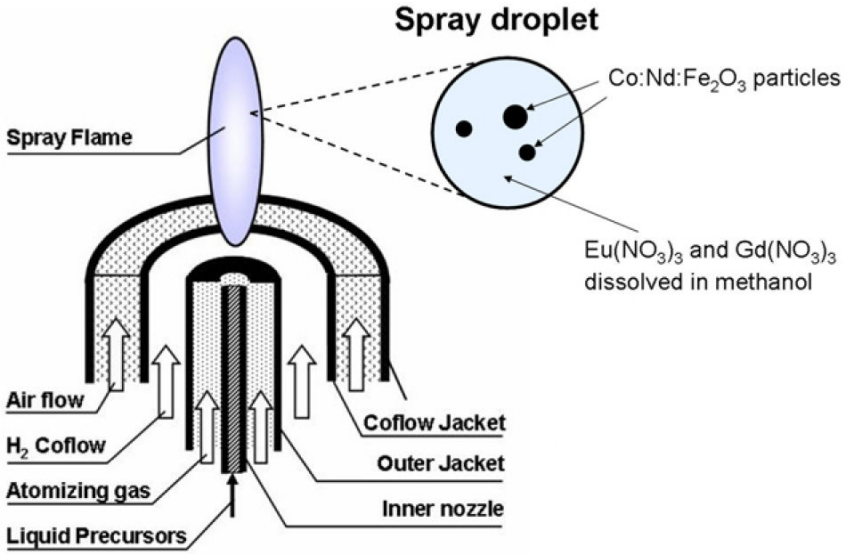

Figure 2.
Schematic description of the synthesis of core /shell particles. Spray droplets contain solid magnetic nanoparticles and dissolved precursors of Eu and Gd passed through the hydrogen flame.

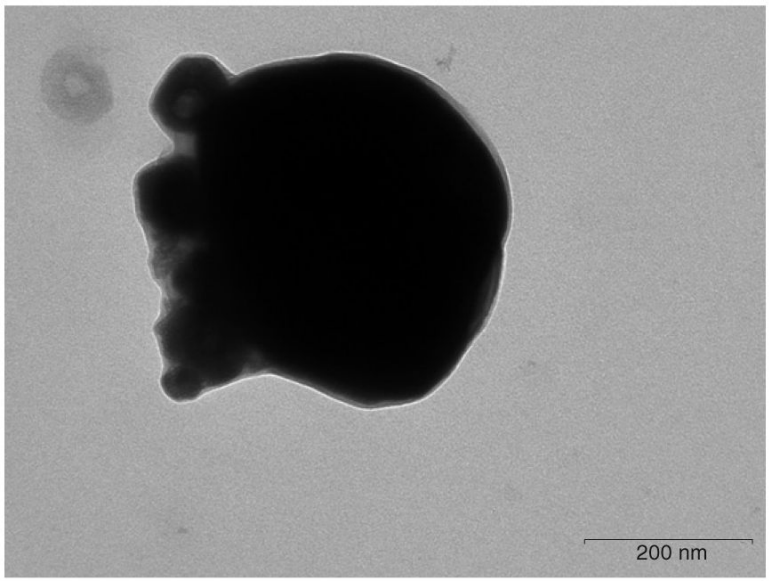

Figure 3.
Bright field TEM image of Co:Nd:Fe_2O_3/Eu:Gd_2O_3 core/shell particles.

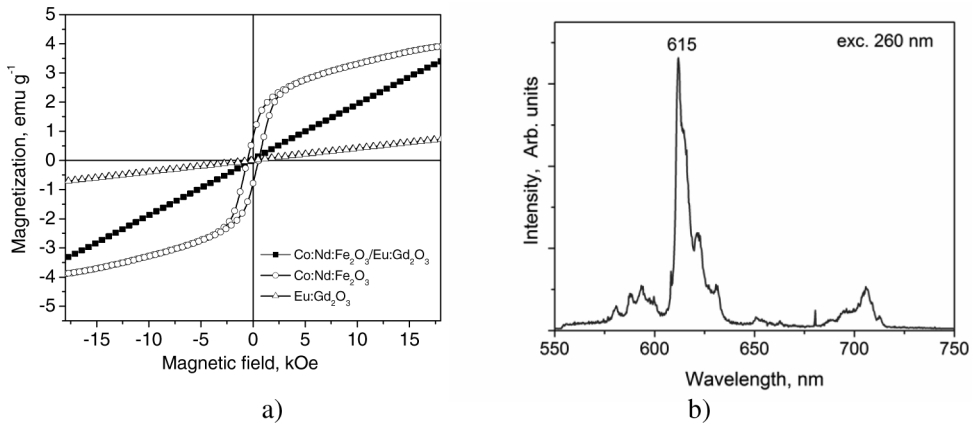

Figure 4.

Properties of the magnetic/luminescent core/shell particles. (a) Comparison of the magnetic characteristics of Co:Nd:Fe_2O_3 powder with Co:Nd:Fe_2O_3/Eu:Gd_2O_3 core/shell particles and Eu:Gd_2O_3 particles; (b) emission spectrum of the Co:Nd:Fe_2O_3/Eu:Gd_2O_3 core/shell particles under excitation at 260 nm.

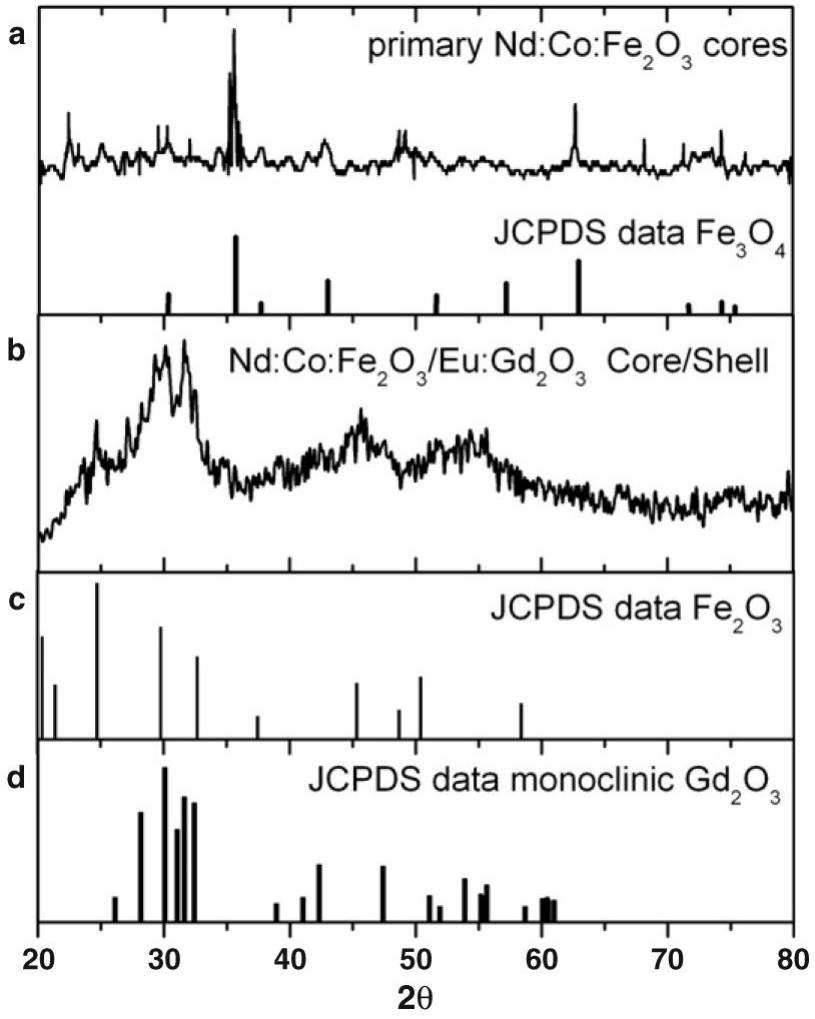

Figure 5.

(a) X-ray diffraction spectrum of the primary Nd:Co:Fe_2O_3 particles are compared to the typical XRD peaks of Fe_3O_4; (b) XRD of the core/shell Nd:Co:Fe_2O_3/Eu:Gd_2O_3 particles; (c) and (d) show the typical XRD spectral peaks of Fe_2O_3 and monoclinic Gd_2O_3 respectively.

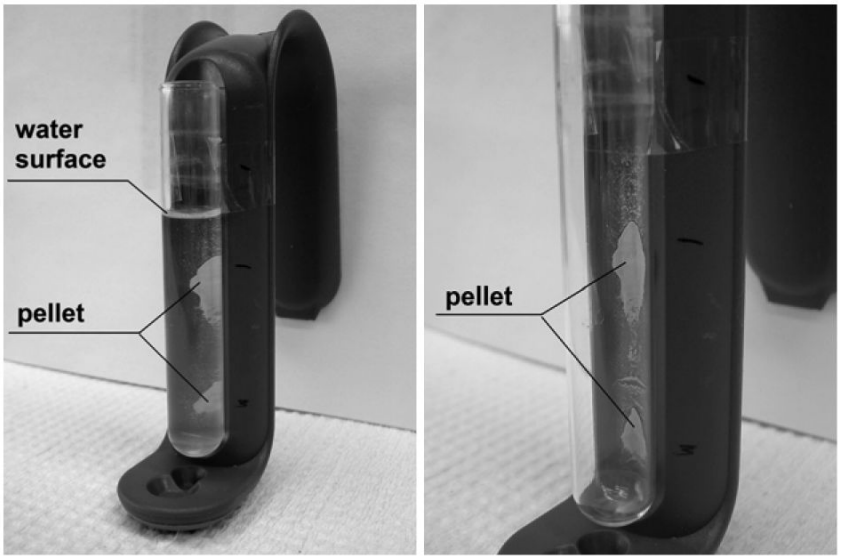

Figure 6.
Magnetic separation of Co:Nd:Fe_2O_3/Eu:Gd_2O_3 particles from aqueous solution; (left)—before the liquid is removed, (right)—after removing the liquid.

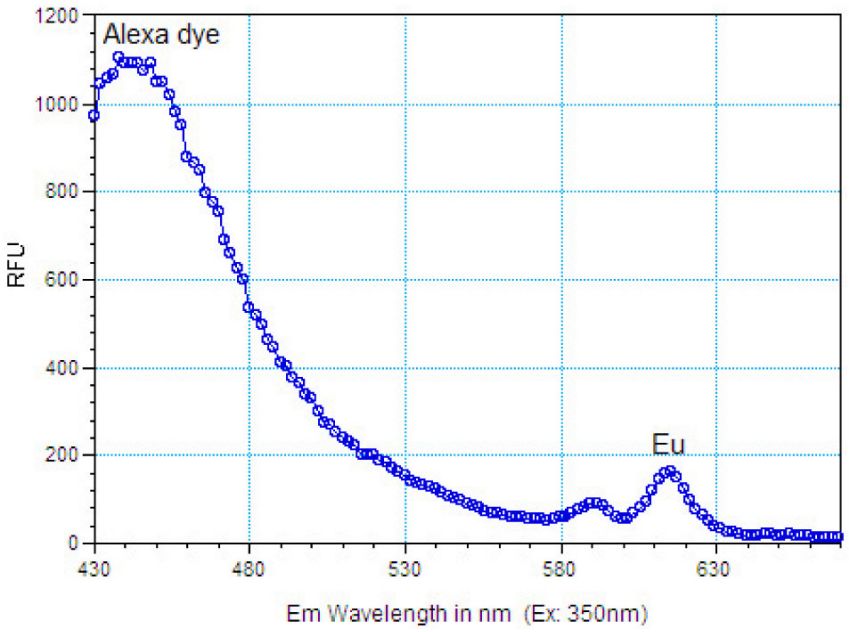

Figure 7.
Emission spectra of the Co:Nd:Fe_2O_3/Eu:Gd_2O_3 core/shell particles and the IgG-Alexa Fluor 350 bound to their surface (excitation at 350 nm).

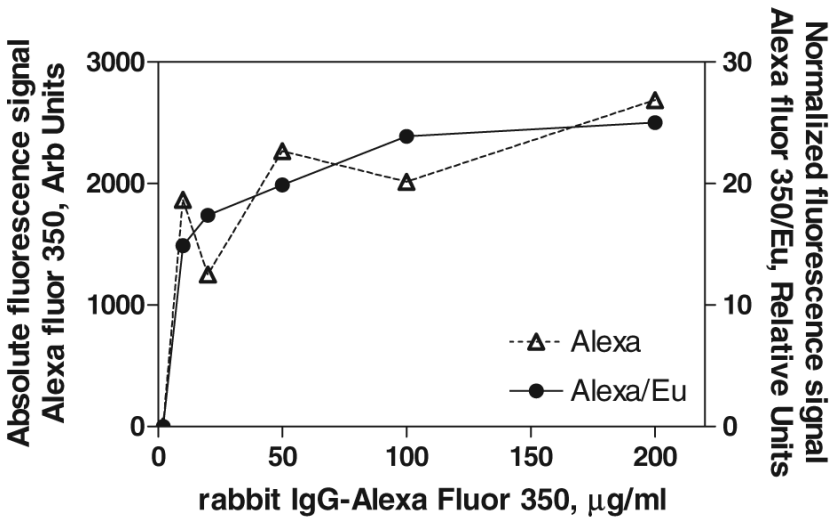

Figure 8.

Saturation of the capture antibody (anti-rabbit IgG) immobilized on the surface of the magnetic luminescent nanoparticles with rabbit IgG-Alexa Fluor 350. Absolute measured intensity of the Alexa peak (△) is compared to the intensity ratio Alexa/$EuGd_2O_3$ (●). The ratiometric approach reduces the uncertainty that arises from variations in the amount of particle separation from the sample with the magnet.

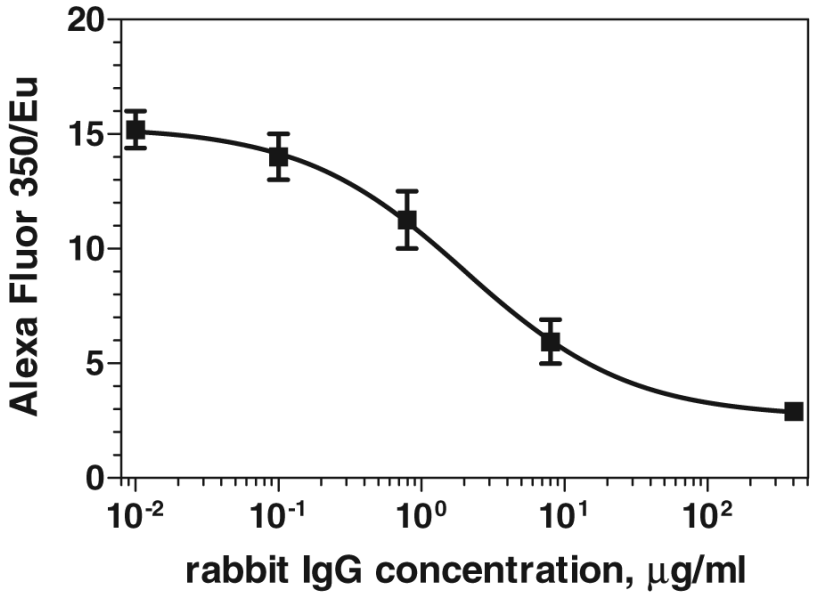

Figure 9.
Calibration curve for the competitive magnetic immunoassay for rabbit IgG. The signal of the labelled antigen (rabbit IgG-Alexa Fluor 350) bound on the surface of the magnetic nanoparticles is normalized by the Eu luminescence of the particles.